6ICEGE 6th International Conference on Earthquake Geotechnical Engineering
1-4 November 2015
Christchurch. New Zealand

A Centrifuge Study: Influence of Base Fixity on the Seismic Response of Buried Reservoir Structures

A. Hushmand[1], S. Dashti[2], C. Davis[3], B. Hushmand[4], M. Zhang[5], Y. Lee[6], J. Hu[7]

ABSTRACT

A series of centrifuge experiments were conducted at the University of Colorado Boulder to evaluate seismic soil-structure-interaction, lateral earth pressures, bending strains, moments, and racking displacements of scaled model structures representing water reservoirs buried in medium dense, dry sand and dense silty sand. This paper focuses on the influence of base fixity on the seismic performance of an underground structure restrained from rotation at the roof and floor levels. The preliminary results indicate that underground structures similar in type to those tested in this study can experience seismic lateral earth pressures of engineering importance. Fixing the base of the structure was observed to amplify earth pressures near the base. None of the available analytical methods predicted the shape and magnitude of seismic lateral earth pressures accurately. The insight from these tests is useful in understanding the performance of underground reservoir structures worldwide.

Introduction

The current state of practice for the seismic design of underground reservoir structures relies heavily on simplified analytical methods or numerical tools that have not been calibrated or validated adequately against physical model studies for a range of conditions. The kinematic constraints of these structures are not fully captured by simplified seismic analysis procedures. Soil-structure-interaction (SSI) near these structures is complex and depends on foundation fixity, properties of the surrounding soil, flexibility of the structure relative to soil, and the characteristics of the earthquake motion.

Traditionally, underground structures are categorized either as *yielding* or *rigid-unyielding*, and designed accordingly. The current state of practice for assessing seismic earth pressures on *yielding* structures relies heavily on the methods developed by Mononobe-Okabe (Okabe 1926; Mononobe and Matsua 1929) and Seed-Whitman (1970). For *rigid-unyielding* walls, the method of choice is often the simplified solution proposed by Wood (1973), which assumes fully rigid walls (no flexural wall movement). Underground reservoir structures fall in between the two extreme cases of *yielding* and *rigid-unyielding*, because they are not fully rigid (exhibit some deformation), but their wall deformation is limited as they are stiff and are restrained at their base and roof. In this paper, these reservoir structures are classified as *stiff-unyielding* structures.

[1]PhD Student, Civil Eng., Univ. of Colorado Boulder, Boulder, CO, USA, ashkaan.hushmand@colorado.edu
[2]Assistant Professor, Civil Eng., Univ. of Colorado Boulder, Boulder, CO, USA, shideh.dashti@colorado.edu
[3]Trunk Line Design Manager, Los Angeles Department of Water and Power, CA, USA, craig.davis@ladwp.com
[4]President and Principal Engineer, Hushmand Associates, Inc., Irvine, CA, USA, ben@HAIEng.com
[5]Centrifuge Engineer, Civil Eng., Univ. of Colorado Boulder, Boulder, CO, USA, mizh8380@colorado.edu
[6]Civil Engineering Associate, Los Angeles Department of Water and Power, CA, USA, yangsoo.lee@ladwp.com
[7]Civil Engineering Associate, Los Angeles Department of Water and Power, CA, USA, jianping.hu@ladwp.com

A series of centrifuge tests were conducted at the University of Colorado Boulder centrifuge facility to study the seismic response of *stiff-unyielding* underground structures buried in different types of cohesionless soils. The model structures represented prototype reinforced concrete reservoirs with 11 to 12 m walls and restrained against rotational movement at their roof and floor levels. This paper presents the results of two centrifuge experiments with the same structure and soil type, but different base fixities and soil heights, to investigate their effects on accelerations, lateral earth pressures, and bending strains acting on the structure walls.

Experimental Setup

Two centrifuge experiments were performed at 60 g of centrifugal acceleration using the 400-g ton centrifuge at University of Colorado Boulder. As shown in
Figure 1, in the baseline centrifuge test (T-BL), the model structure was placed on about 8 m of soil (in prototype scale), whereas in a second test (T-Fixed), the same structure was attached to the base of the container. The tests were conducted in a transparent flexible shear beam (FSB) container developed by Ghayoomi et al. (2013). The internal dimensions of the FSB container were 337 mm in height, 305 mm in width, and 699 mm in length. The cross section view of experiments T-BL and T-Fixed with instrumentation layout is shown in
Figure 1.

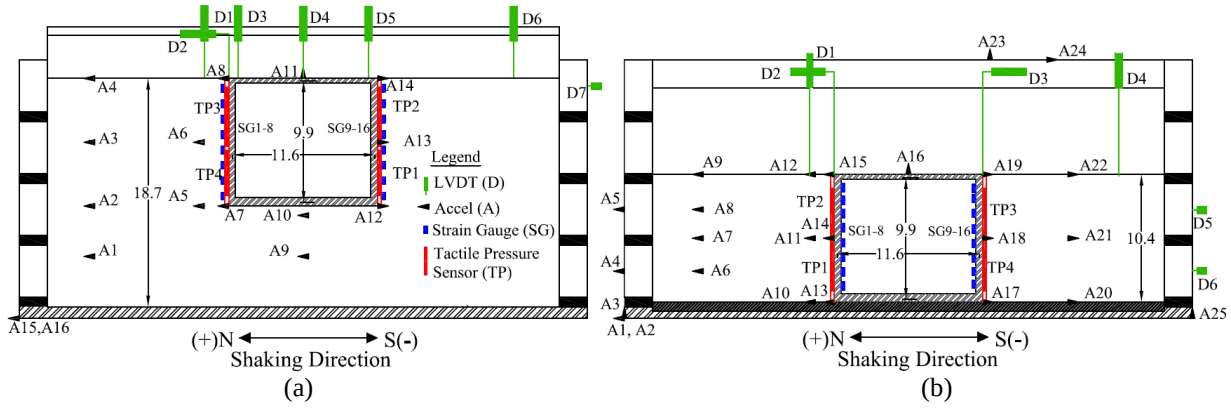

Figure 1. Cross-section views of centrifuge tests: (a) T-BL and (b) T-Fixed (dimensions shown in prototype scale meters).

The model structures tested were simplified versions of the actual prototype reservoirs considered by the Los Angeles Department of Water and Power (LADWP), which are complex structures with many columns and interior walls. The structures were designed to match the mass, lateral stiffness, and natural period of the target prototype reservoir structures. The model structures were constructed of 1018 Carbon Steel (density = 7870 kg/m3; Young's Modulus = 2e8 kPa). Table 1 summarizes the dimensions, lateral stiffness, and natural frequency of the baseline structure that is presented in this paper. Uniform Nevada Sand No. 120 (G_s=2.65; e_{min}=0.56; e_{max}=0.84; D_{50}=0.13 mm; C_u=1.67) was dry pluviated into the FSB container to achieve a $D_r \approx 60\%$ (dry unit weight $\approx$ 15.56 kN/m^3). A series of five horizontal earthquake motions were applied to the base of the models in the same sequence in the two experiments, as summarized in Table 2. Data was acquired using accelerometers, LVDTs, strain gauges, and

tactile pressure transducers. Lateral earth pressures were measured using model 9500 tactile pressure transducers manufactured by Tekscan Inc. Each tactile sensor contains 14 rows and 14 columns of sensels (sensing points) amounting to 196 sensels, each 5.1 mm by 5.1 mm. Each of the 196 sensels recorded pressure data at a rate of 4,000 samples/sec during the dynamic centrifuge tests.

Table 1. Dimensions and properties of model structure (model scale).

Height & Width (cm) Center to Center	Thickness			Lateral Stiffness, K_L (kN/m/m)	Fundamental Frequency (Hz)	
	Base (cm)	Roof (cm)	Wall (cm)		Numerical	Experimental
16.52 & 19.3	1.15	0.62	0.93	0.15	238	232

Table 2. Base earthquake motion properties as recorded during T-BL by accelerometer A15 (all units in prototype scale).

Ground Motion Name	PGA (g)	Arias Intensity I_a (m/s)	Significant Duration $D_{5\text{-}95}$ (s)	Mean Period T_m (s)	Predominant Period T_p (s)
Northridge-L	0.36	1.6	15.4	0.71	0.35
Northridge-M	0.81	5.4	19.5	0.66	0.28
Northridge-H	1.2	11.6	25.1	0.63	0.28
Izmit	0.33	2.1	39.5	0.56	0.24
Loma	1.0	12.4	13.3	0.50	0.27

Experimental Results

Acceleration Recordings

Accelerometers A15 (T-BL) and A-20 (T-Fixed) measured the ground motions at the base of the FSB container. The achieved base motions were slightly different in the two experiments, because of the large difference in model weight and modal frequencies. Figure 2 compares the spectral accelerations of the base motions in T-BL and T-Fixed. The “free-field” ground motion amplification away from the structure is compared between the two tests during the Northridge-L and Izmit motions in Figure 3. Slightly more amplification is observed at higher frequencies in T-Fixed with a higher site fundamental frequency. The ground motion amplification patterns at the base, middle, and top of the structure wall are compared in T-BL and T-Fixed during different motions in Figure 4. This figure indicates an amplification of structural accelerations at higher frequencies in T-Fixed compared to T-BL, particularly near the top with less confinement.

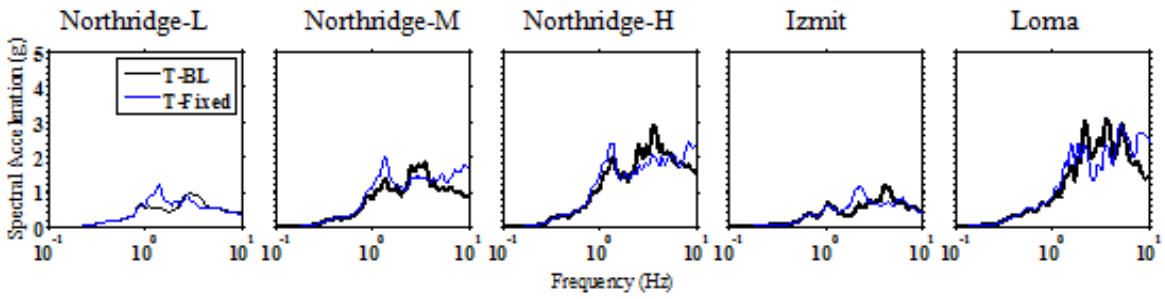

Figure 2. Base motion spectral accelerations (5% damped) in T-BL and T-Fixed.

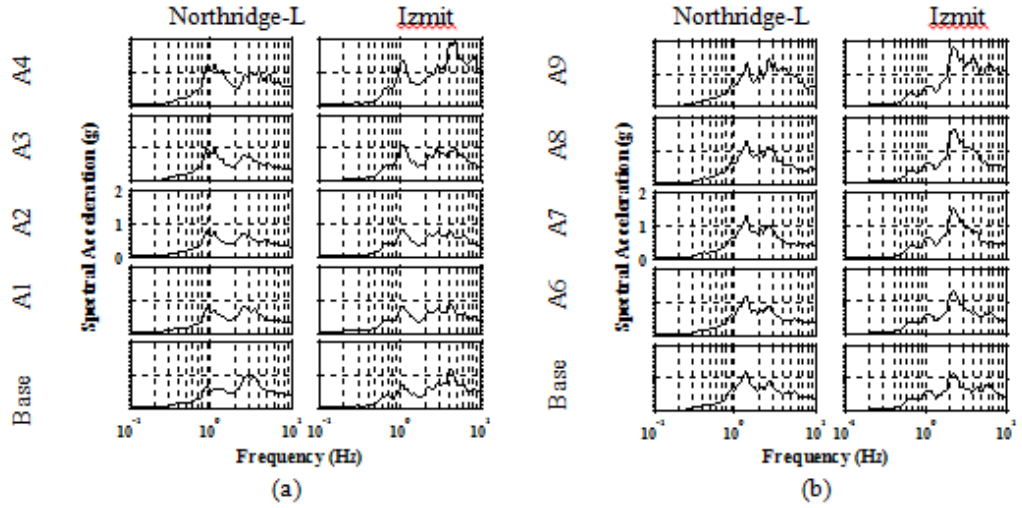

Figure 3. Amplification of spectral accelerations in the free-field in: a) T-BL; b) T-Fixed.

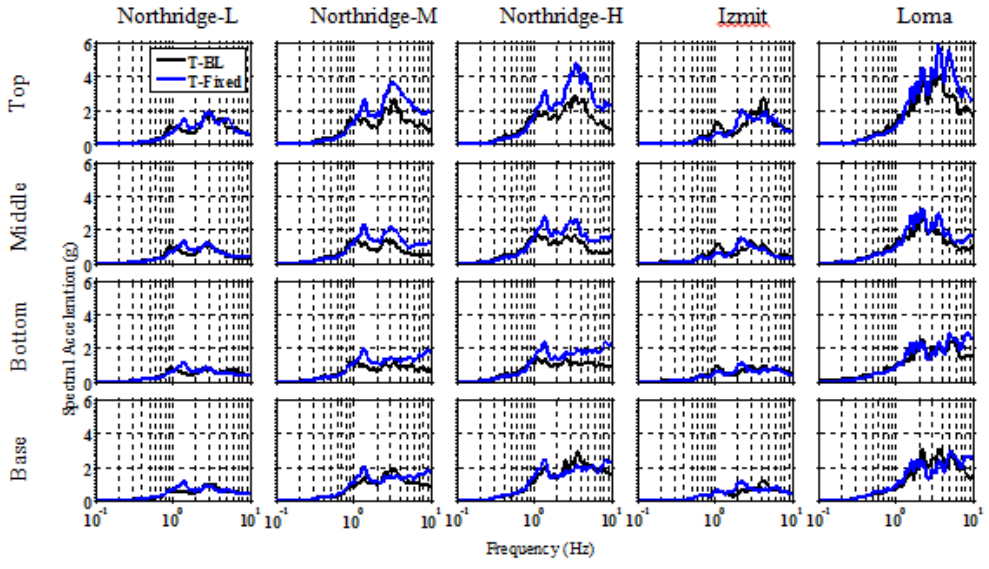

Figure 4. Spectral accelerations (5% damped) on the structure in T-BL and T-Fixed.

Lateral Earth Pressures

To reduce scatter, the pressure recordings obtained from nine adjacent sensels were averaged to represent a larger sensing area, after removing the non-working and outlier sensels. Nine-cell averaging reduced the tactile sensor recordings from a matrix of 14x14 to 12x12. Then, each row was averaged to obtain a matrix of 12 x 1 pressure time histories. This method was successful in reducing the scatter in pressure recordings, particularly when in contact with granular materials with local inhomogeneities. Then, after applying static and dynamic calibration factors (Gillis et al. forthcoming), each row was subjected to a band-pass, 5^{th} order, a-causal, butterworth filter with corner frequencies of 0.1 and 15 Hz, to remove low and high frequency noise. It must be noted, however, that obtaining reliable pressure recordings in centrifuge is a topic of ongoing investigation. Even though significant improvements were made in the installation, calibration, and processing of these sensors, their results should be evaluated with caution.

The dynamic increment of thrust was calculated by numerically integrating the dynamic increment of pressure along the height of the wall at each time step. The resulting dynamic thrust time histories in T-BL and T-Fixed during the Northridge-L motion are compared in Figure 5.

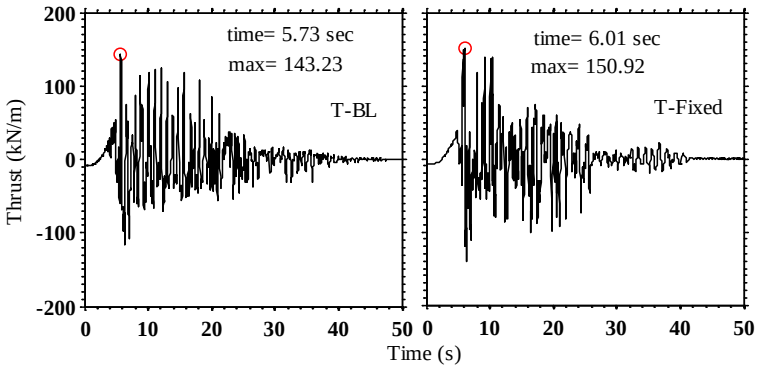

Figure 5. Dynamic thrust time histories during the Northridge-L motion in T-BL and T-Fixed.

The thrust time histories were similar during the two tests, but slightly larger in T-Fixed during this motion. Figure 6 shows the Fourier Amplitude Spectra of dynamic thrust compared to those of acceleration at the mid-depth of the structure wall during all motions. The frequency content of dynamic thrust was similar to that of structure acceleration in T-BL during all motions. In T-Fixed, however, dynamic thrust showed a higher content at lower frequencies (about 0.3 to 1 Hz) compared to the mid-structure acceleration. Overall, the amplitude of dynamic thrust was comparable in the two tests, with the exception of the Northridge-M motion, where dynamic thrust showed a significantly greater content in T-Fixed in frequencies ranging from about 0.6 to 0.9 Hz compared to T-BL.

Figure 7 shows the static, pre-shake, and post-shake lateral earth pressure and the total (static and dynamic) pressure profiles at the time corresponding to maximum thrust during the Northridge-L event in each test. The plot also includes the theoretically expected range of static, at-rest (K_o conditions) and active (K_a) lateral earth pressures for comparison. A friction angle of approximately 35^o was assumed for Nevada Sand in these experiments (Popescu 1993). Both

tests showed a reasonable trend in static earth pressure recordings. The dynamic earth pressures at the time of maximum thrust were not negligible in either test, even during the Northridge-L event with a base PGA of about 0.36 g.

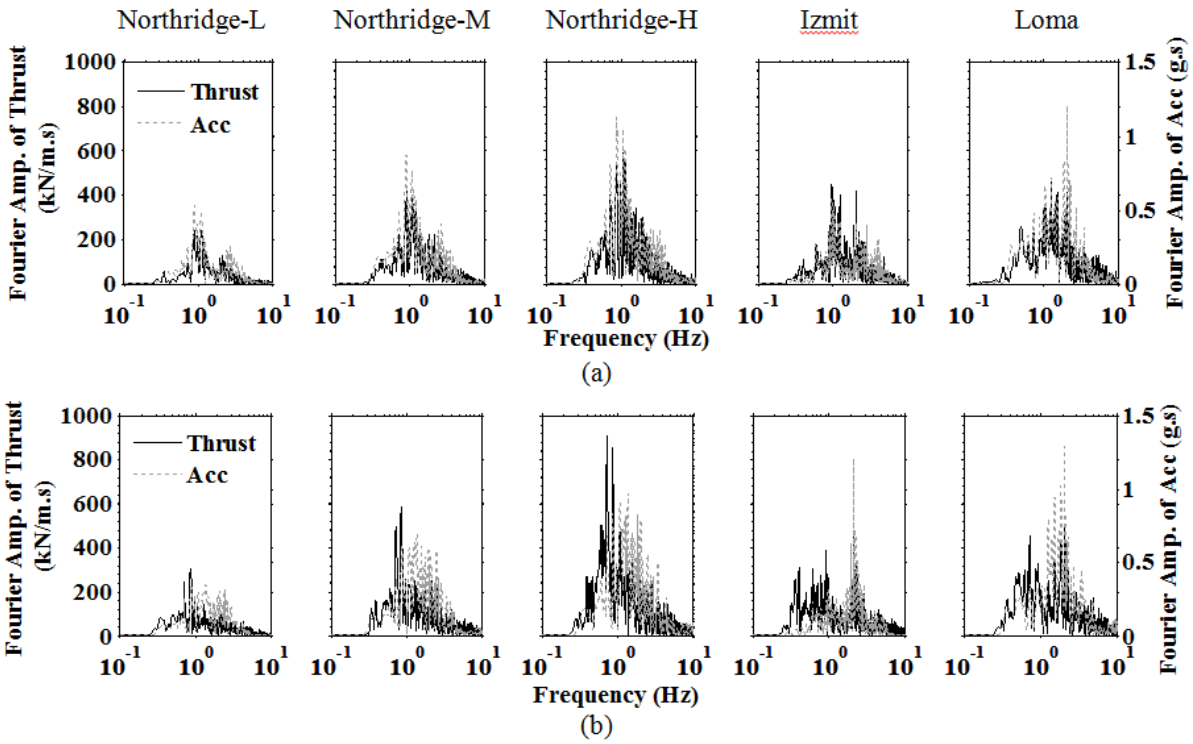

Figure 6. Fourier Amplitude Spectra of dynamic thrust and mid-depth structure acceleration in: (a) T-BL; (b) T-Fixed.

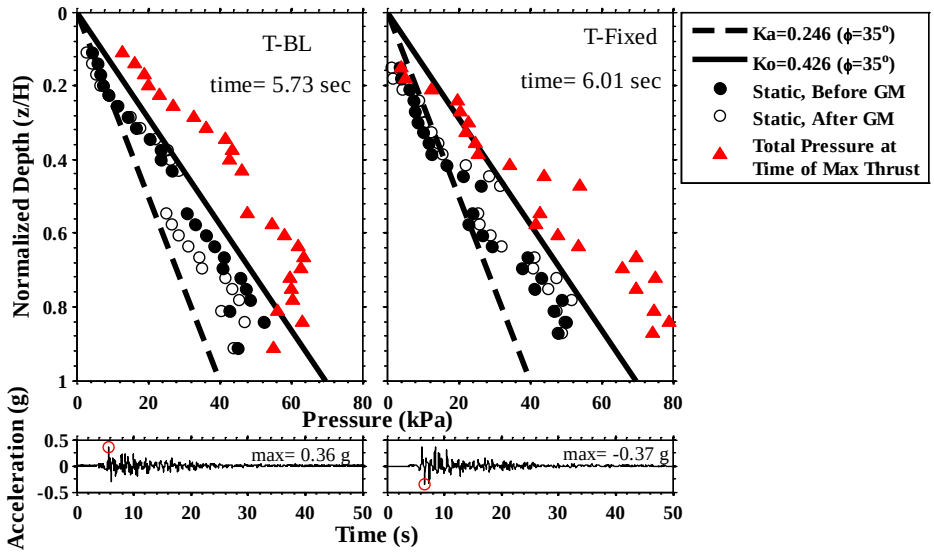

Figure 7. Static (before and after the ground motion) and total (static and dynamic) lateral earth pressures at the time of maximum thrust in T-BL and T-Fixed during the Northridge-L motion.

The dynamic increment of pressure profile ($\Delta\sigma_E$) is shown in Figure 8 along with the simplified methods of Mononobe-Okabe (M-O), Seed and Whitman (S-W), and Wood in T-BL and T-fixed during all motions. The PGA of the free-field surface accelerometer was used to obtain the horizontal acceleration coefficient (k_h) in the different analytical methods. The M-O solution is not shown in the Northridge-H and Loma ground motions because it is indeterminate for PGA values greater than 0.7g for a soil friction angle of 35°. The $\Delta\sigma_E$ was calculated using Wood's simplified method for a backfill length to wall height ratio (L/H) of 1.5 corresponding to the centrifuge test and also a greater L/H ratio of 10 as an upper bound for comparison. Wood's simplified method overestimated the pressure at shallow depths, since it does not take into account an increase in soil shear modulus with depth. The measured $\Delta\sigma_E$ values on the upper half of the wall roughly followed the M-O solution in terms of both amplitude and shape. Overall, the results showed that none of the theoretical methods capture the trends seen in the measured $\Delta\sigma_E$ data.

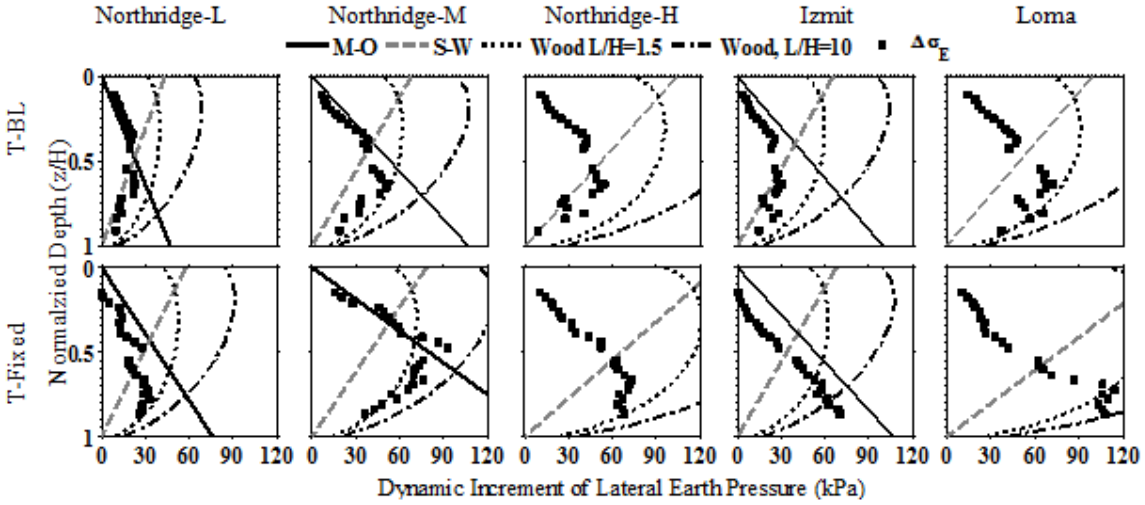

Figure 8. Dynamic lateral earth pressures at the time of maximum thrust in T-BL and T-Fixed.

The shape of the $\Delta\sigma_E$ profiles measured on the wall varied in T-BL and T-Fixed. In T-BL the shape was more rounded with the maximum $\Delta\sigma_E$ occurring near the center of the height of the wall. The $\Delta\sigma_E$ values increased near the bottom of the wall in T-Fixed compared to T-BL in most cases, likely because of a greater energy transmitted to the structure with a fixed connection allowing no slippage at its base and increasing structure inertia compared to the surrounding soil.

Bending Strains

Total bending strains were measured on the walls of the structure by wiring the strain gages in a half bridge configuration. The dynamic increment of bending strain ($\Delta\varepsilon_E$) on both walls showed similar trends and magnitudes. Hence only the $\Delta\varepsilon_E$ profiles are shown on one wall at the time of maximum $\Delta\varepsilon_E$ in Figure 9. The shape of the $\Delta\varepsilon_E$ profile was roughly linear in both tests during all motions, with peaks near the fixed connections with roof and base of the reservoir structure. The magnitude of $\Delta\varepsilon_E$ in T-Fixed was overall larger than T-BL especially near the base of the structure.

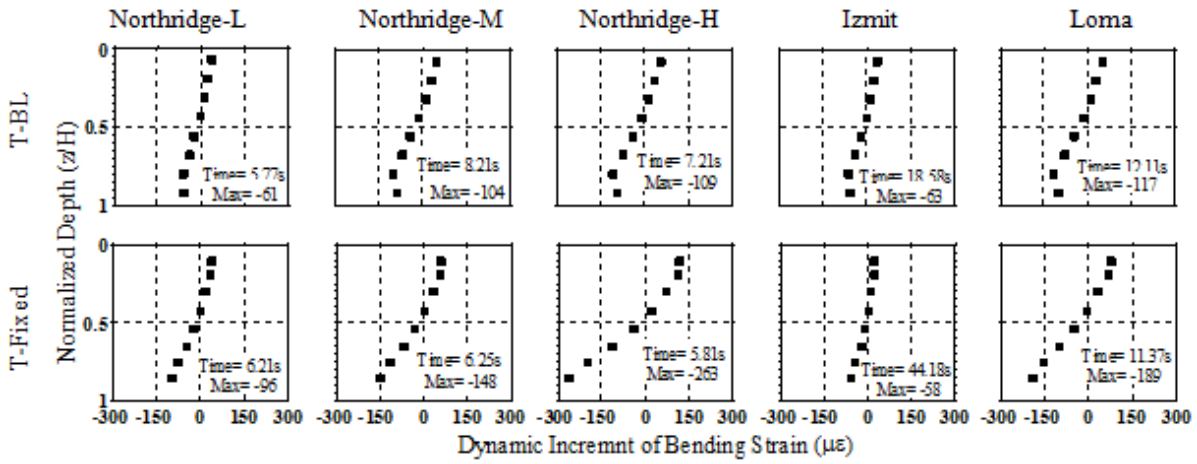

Figure 9. Dynamic increment of bending strains ($\Delta\varepsilon_E$) at the time of maximum strain in T-BL and T-Fixed.

Conclusions

In this paper, we present the results of two centrifuge experiments that investigate the seismic response of *stiff-unyielding* buried reservoir structures in medium dense, dry sand and the influence of base fixity and earthquake motion properties on accelerations, lateral earth pressures, and bending strains. The preliminary results indicate that underground structures similar in type to those tested in this study can experience seismic lateral earth pressures of engineering importance, even during weaker motions with base PGA of approximately 0.3g. Fixing the base of the buried structure was observed to amplify pressures near the base and bending strains in some cases. None of the available simplified methods predicted the shape and magnitude of seismic lateral earth pressures accurately. The insight from these tests is useful for understanding the performance of underground reservoir structures worldwide.

References

Ghayoomi M, Dashti S, McCartney JS. Performance of a transparent Flexible Shear Beam container for geotechnical centrifuge modeling of dynamic problems. *Soil Dyn. and EQ Engineering* 2013; **53**, 230-239.

Mononobe N, Matsuo M. On the determination of earth pressures during earthquakes. *Proc. World Engineering Congress* 1929; Vol. 9: 179-187

Okabe S. General theory of earth pressure. *Journal of the Japanese Society of Civil Engineers* 1926; Vol. **12**

Popescu R, Prevost JH. Centrifuge validation of a numerical model for dynamic soil liquefaction. *Soil Dyn. and EQ Engineering* 1993; **12**(2), 73-90.

Seed HB, Whitman RV. Design of earth retaining structures for dynamic loads. *ASCE Specialty Conference, Lateral Stresses in the Ground and Design of Earth Retaining Structures* 1970; 103-147

Wood JH. *Earthquake Induced Soil Pressures on Structures.* PhD Thesis 1973; Calif. Inst. of Tech., Pasadena, CA.